A novel method for combination of ionic conductivity and pH-metry methods for the determination of the aqueous solubility of a new diisopropylammonium hydrogenmaleate crystalline molecule

UNDER PEER REVIEW

ABSTRACT:

Dissociation constant, solubility, and thermodynamic data are very important physicochemical parameters for biological substances and their knowledge is of fundamental importance for the validation of drugs. In addition to their low cost and accessibility, Conductometric and pH-metric methods seem to be particularly suitable for the determination of these parameters given the often weak acidic or basic nature of drugs. These parameters were determined for a new synthesized diisopropylammonium hydrogenmaleate (*i*Pr_2NH_2-MA) crystalline molecule. Conductometric and pH-metric methods were used for this characterization. The pH-metric method lead to pK_{a1} = 3.6, pK_{a2} = 6.7 and pK_{a3} = 7.5, while the conductometric method made it possible to determine two pK_a values which are pK_{a1} = 3.5 and pK_{a3} = 7.8. The values of the thermodynamic parameters calculated for the enthalpy change (Δ_rH^0) and the entropy change (ΔS) of the *i*Pr_2NH_2-MA acidic dissociation reaction are of the order of ΔH = 25. 36 ± 0.06 kJ.mol^{-1} and ΔS = 6.08 ± 0.18 kJ.mol^{-1}.K^{-1}. In addition, the Gibbs free energy change (ΔG) of the molecule decreased as a function of temperature. The solubility varied between 1 and 84 mg mL^{-1} for pH values comprised between 3.5 and 8.5 and reached its maximum S_{max} = 84 mg mL^{-1} at pH 5.6. The dissociation process was found to be is non-spontaneous, endothermic and entropically favorable. These results demonstrated on the one hand the reliability and effectiveness of the Conductometric and pH-metric methods for the characterization of molecules with acidic and/or basic sites, and on the other hand the excellent physical and chemical properties of diisopropylammonium hydrogenmaleate (*i*Pr_2NH_2-MA) crystalline molecule.

Keywords: *Diisopropylammonium hydrogenmaleate, pH-metric method, conductometric method, physicochemical parameters*

1. INTRODUCTION

Foods and medicines include considerable amounts of maleates. These are important pharmacophores in modern drugs due to their ability to improve the physicochemical properties of drugs, such as water solubility. This parameter is a key factor in ensuring better bioavailability of active pharmaceutical ingredients (APIs), and then greater drug efficacy at low dosage. The use of maleate derivatives is therefore extremely important in the development of a new drug because it governs solubility, absorption, distribution, metabolism and elimination [1]. For this, maleate derivatives remain among the most used agents in the design of active pharmaceutical ingredients (APIs) because of it increases the APIs solubility. Recently, timolol maleate was developed and validated as a safe and effective API in the treatment of ocular glaucoma [2,3]. Enalapril maleate has been successfully designated and evaluated according to the United States Pharmacopoeia (USP) for the treatment of hypertensive diseases [4]. Given the growing need to improve the physicochemical properties of research and development compounds, recent decades we have seen the use of a wider variety of new maleate derivatives [5-9].However, it should be noted that maleate derivatives include acidic or basic functional groups with pK_a and solubility values that can affect their physicochemical and biological properties. pK_a values also influence the stereochemical and conformational structure, the orientation of nucleophilic and electrophilic attacks, the capacities of intermediates, the activation energy of inorganic reactions and the detection of active centers of enzymatic biochemistry [8]. Thus the determination of parameters such as pka values, solubility and dissociation constants, the enthalpy ($\Delta_r H^0$) and entropy (ΔS) changes as well as Gibbs free energy (ΔG) becomes necessary for any candidate maleate-derived counterions.

There are several methods for determining dissociation constants such as UV-vis absorption spectroscopy [9-11] , liquid chromatography [10,12], capillary electrophoresis [1314,15], NMR [16], voltammetric methods [17,18], and computational method [19].

These techniques present often the disadvantages due to the use of organic solvents. For example, the liquid chromatography technique has a range of pKa values is often limited by the stability of the column packet. In addition, due to the long retention times observed, it is not easy to determine the pKa values in water and aqueous solutions - organic mixtures with a low content of organic solvent [20].

Traditionally, the pH-metric and conductimetric methods [21] are seen as very useful techniques for determining pK_a values, because of their precision and reproducibility. These methods are high precision techniques to determine the pKa values of the substances. They are commonly used due to its precision and availability of these instruments at low cost.

Recently, Seye and collaborators [22] have synthesized for the first time a new diisopropylammonium hydrogenmaleate crystalline molecule. This diisopropylammonium has been obtained using the diisopropylammine which was used recently with dichloroacetate as being alleviates liver fibrosis through inhibiting activation and proliferation of hepatic stellate cells [23]. This crystalline molecule turns out to have a very high solubility compared to those developed in the literature [24,25].

UNDER PEER REVIEW

In the present work, the pKa values and the thermodynamic parameters of a new diisopropylammonium hydrogenmaleate crystalline molecule have been determined in aqueous medium. These parameters associated with the solubility were determined by conductometry and pH-metry method.

2. EXPERIMENTAL SECTIONS

2.1. Reagents

Maleic acid ($HO_2CH = CHCO_2H$, 99% m/m), diisopropylamine (iPr_2NH, 99% m/m) and, spectroscopic-grade methanol were purchased from Sigma Aldrich and used without purification. Hydrochloric acid (37% m/v) and sodium hydroxide pellets (97% m/m) were supplied by Sigma-Aldrich and used as received. All aqueous solutions were prepared by using Milli-Q ultrapure water (MQ 18.2 MΩcm).

2.2 Materials

According to the proposed objectives, certain experiments were carried out by pH-metric and conductometric titration using a bench-top VWR pHenomenal and conductivity CON 2700 EUTECH. In both cases, the previous calibration steps were carried out using solutions and buffers suitable for room temperature (25 ± 1 ° C).

The VWR pHenomenal, bench-top, was equipped with a glassy electrode with integrated temperature sensor 22, a LCD screen showing the pH / mV and temperature values simultaneously, and three additional technical buffers at 25 ° C (4.00 / 7.00 / 10.00) in memory. The CON 2700 EUTECH bench-top conductivity meter was equipped with a digital screen, a conductivity cell, an electrode holder stand and automatic recognition of standards.

The temperature variations were made possible by a magnetic heating stirrer called the IKA Plate (RCT digital) including a circular aluminum alloy heating plate. The weighing was made using a Metler PM 100 balance.

2.3 Measurement procedure

All the titrations were carried out by adding appropriate quantities of titrating solutions to samples of iPr_2NH_2-MA with constant and slight agitation. Depending on the reaction to be carried out, the concentrations of the samples and standards were optimized in order to better exploit the analytical signals. The samples are estimated between 45 and 50 mL in order to be able to completely soak the electrodes in order to minimize measurement errors.

3. RESULTS AND DISCUSSIONS

3.1 Synthesis and characterization of diisopropylammonium hydrogenmaleate (iPr_2NH_2-MA)

The scheme 1 represent the procedure for synthesis of $iPr_2NH_2O_2C$-CH = CH-CO_2H crystalline molecule and previously reported [22].

UNDER PEER REVIEW

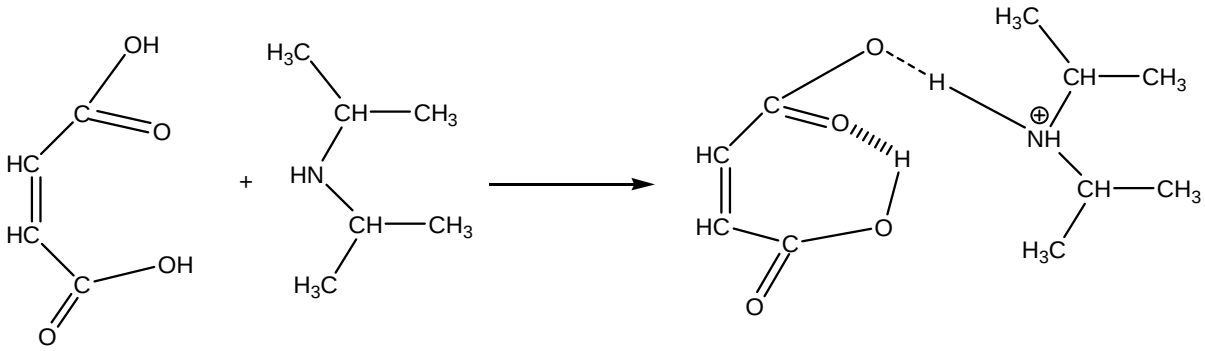

Scheme 1. Procedure for synthesis of *i*Pr_2NH_2-MA

3.2 Proton transfer mechanism of iPr2NH2-MA in aqueous medium

By observing the structure of *i*Pr_2NH_2-MA, it is possible to identify carboxylate, ammonium and carboxylic groups, which suggests possibilities of extraction or transfer of protons depending on the nature of the medium (Schemes 2,3,4). Diisopropylammonium hydrogenmaleate (*i*Pr_2NH_2-MA) behaves like an ampholyte and is composed of three sites that can react according to the nature of the medium: two acid sites (carboxylic and ammonium) and a basic site (carboxylate).

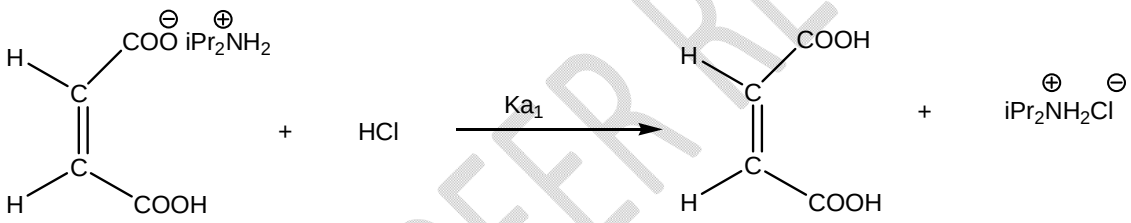

iPr_2NH_2-MA **maleic acid**

Scheme 2. Neutralization of the basic site of diisopropylammonium hydrogenmaleate.

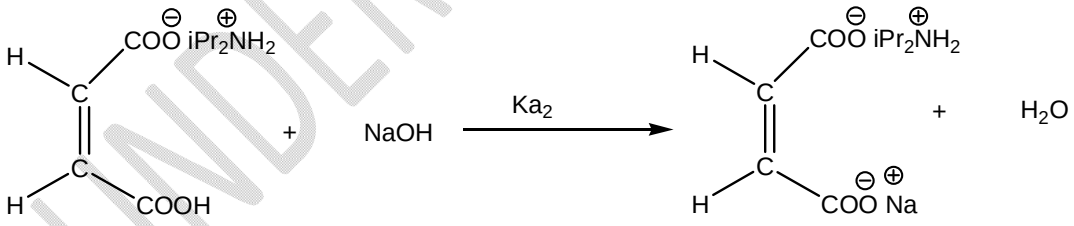

iPr_2NH_2-MA **iPr_2NH_2,Na-MA**

Scheme 3. Neutralization of the first acid site (COOH group).

UNDER PEER REVIEW

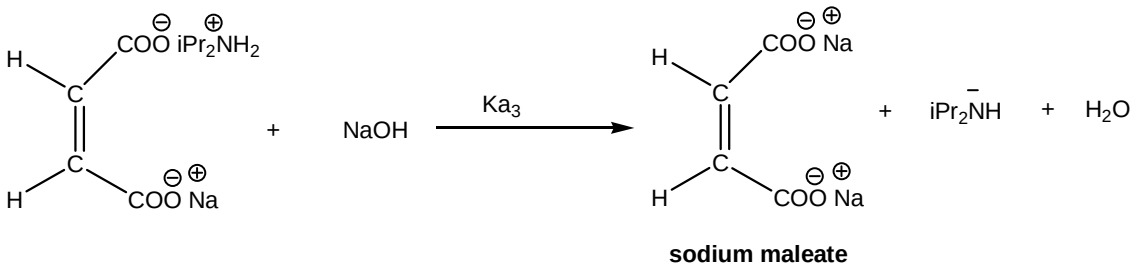

sodium maleate

Scheme 4. Neutralization of the second acid site (ammonium group).

Comparative experimental methods such as pH-metry and conductimetry will make it possible to follow the evolution of *i*Pr_2NH_2-MA in acidic and basic medium.

3.3 pH-metric dosage

In Fig. 1A, we represent the neutralization curve of the basic site (carboxylate) of *i*Pr_2NH_2-MA by HCl. On the other hand, the neutralization curve of *i*Pr_2NH_2-MA with NaOH shows by the appearance of two levels the presence of two acid sites (Fig. 1 B). In fact, as shown in scheme 3, NaOH (strong base) reacts first with the most acidic (carboxylic) site. In the second step, the attack on the last acid site (ammonium) is done in order to completely neutralize the acid sites of the molecule of *i*Pr_2NH_2-MA (Scheme 4).

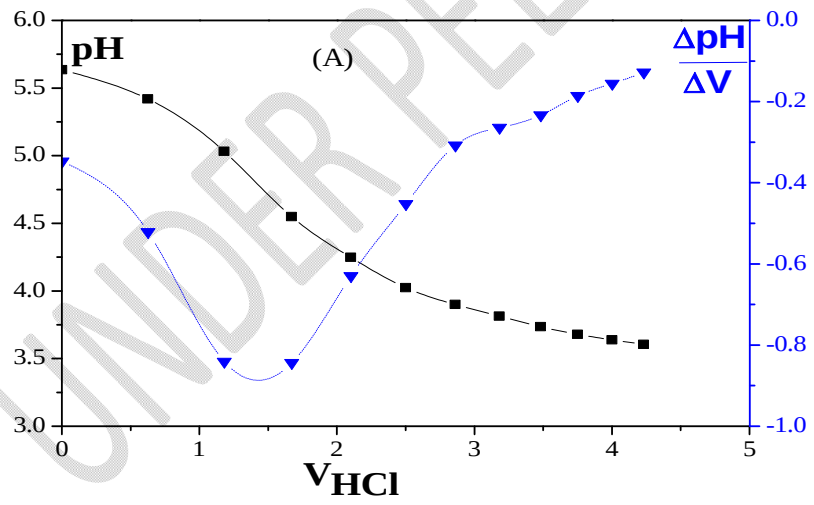

UNDER PEER REVIEW

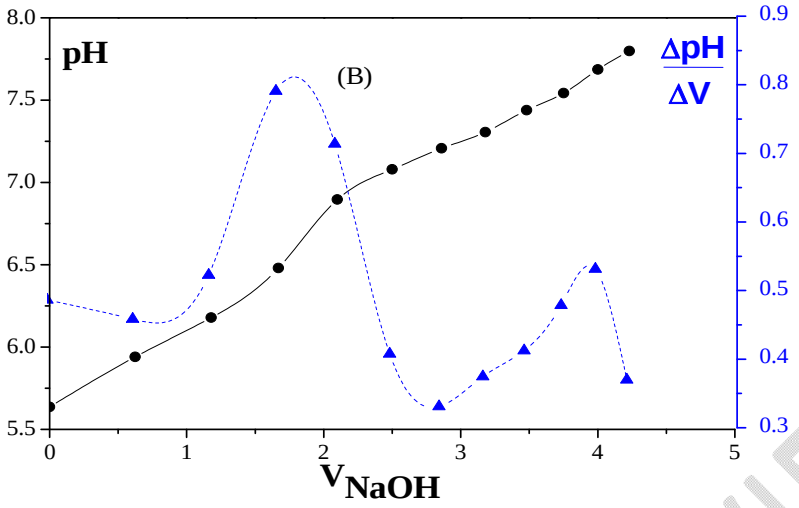

Fig. 1. pH-metric titration curves of 50 mL of *i*Pr_2NH_2-MA and of the first derivative of pH as a function of the volume of A): HCl and B): NaOH.

3.4 Conductometric dosage

Fig. 2 shows the conductivity as a function of the added volume of HCl (10^{-3} mol L^{-1}). The measurements were carried out in *i*Pr_2NH_2-MA solutions (45 mL) of different concentrations (10^{-3}, 4.10^{-4}, 2.10^{-4} and 10^{-4} mol L^{-1}).

The reaction of diisopropylammonium hydrogenmaleate with hydrochloric acid leads to the formation of maleic acid (Scheme 2). It is graphically reflected by an initial drop of the conductivity, which corresponds to a decrease in the concentration of ions present in solution. However, when the maleate is completely neutralized, the addition of HCl in the solution leads to an increase of conductivity. This increase in conductivity is explained by the presence of H^+ ions in the solution due to the addition of non-reacting hydrochloric acid when the maleate is completely neutralized. In addition, the conductimetric method shows that the molecule has a single basic site and confirms the pH-metric technique.

UNDER PEER REVIEW

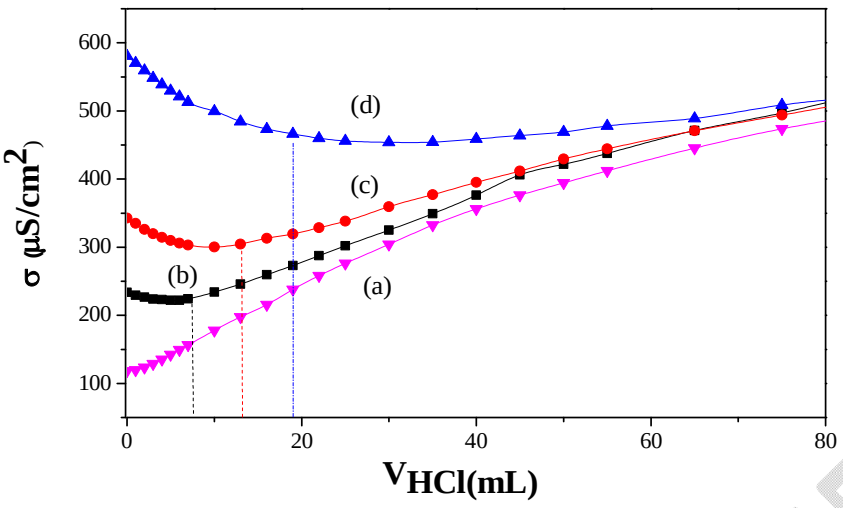

Fig. 2. Conductometric dosage curves for different iPr_2NH_2-MA solutions: a) 10^{-4} mol.L^{-1}; b) 2.10^{-4} mol.L^{-1}; c) 4.10^{-4} mol.L^{-1}; d) 10^{-3} mol.L^{-1} with a solution of 10^{-3} mol.L^{-1} HCl.

For a concentration of 10^{-4} mol.L^{-1}, the addition of HCl directly leads to a continuous increase of the conductivity, signifying an immediate neutralization of the maleate solution by the small volume of HCl added in. By varying the *i*Pr_2NH_2-MA concentration from 2.10^{-4} to 10^{-3} mol.L^{-1}, we observed the appearance of minima on the curves, which correspond to equivalent volume of HCl. The presence one minimum on each curve may be indicative that only one basicity is neutralized.

Fig. 3 represents the experimental results obtained by measuring the conductivity of two solutions of *i*Pr_2NH_2-MA (V = 50 mL) as a function of the added volume of NaOH (10^{-3} mol.L^{-1}). These conductivity curves of *i*Pr_2NH_2-MA solutions ($0.5.10^{-3}$ and $0.8.10^{-3}$ mol.L^{-1}) as a function of the added volume of NaOH have the same appearance and can be divided into three parts.

i) Part materialized by a gradual increase of the conductivity. Indeed, as described above, the strong base NaOH attacks in the first place the most acidic site (Scheme 3) which causes the increase of the charges in solution thus inducing an increase in the mobility of the ions [26] and consequently the conductivity.

ii) The neutralization of the second acid site, accompanied by the transformation of the diisopropylammonium ion into diisopropylamine (Scheme 4), results experimentally in a very small (almost constant) variation of the conductivity in the medium. This result can be explained by the fact that the transformation of the diisopropylammonium ion into a molecule, which would have the effect of reducing the concentration of the ions in the solution, and therefore the conductivity is compensated by the formation of Na^+ ions resulting from the addition of NaOH. We hence obtain an almost constant value of the conductivity during this neutralization reaction of the second acid site.

iii) The last step corresponds to the complete neutralization of the molecule and results in the increasing of Na^+ and OH^- concentrations, leading to a considerable increase of the conductivity in the medium.

UNDER PEER REVIEW

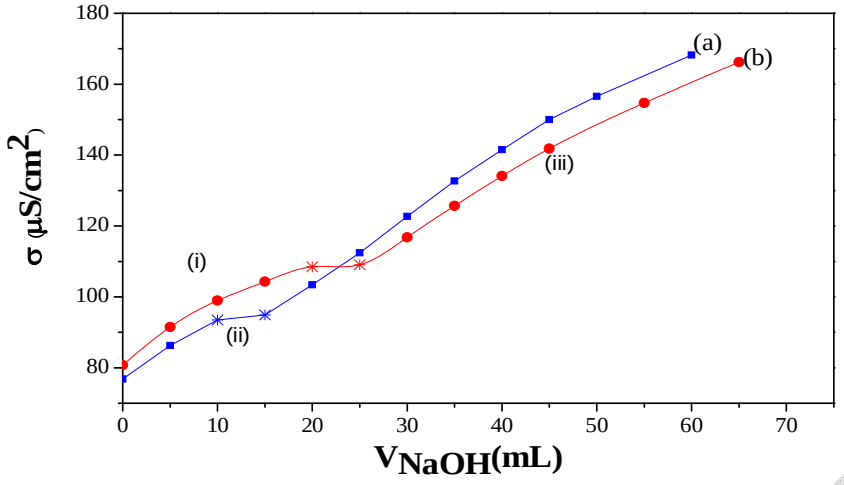

Fig. 3. Conductometric dosage curves for different *i*Pr_2NH_2-MA solutions: a) 0.5x10^{-3} mol.L^{-1} and b) 0.8x10^{-3} mol.L^{-1} using NaOH.

These results obtained confirm the amphoteric character described by the pH-metric method.

3.5 Determination of physicochemical parameters

3.5.1 pK_a values

3.5.1.1 pH-metric method

One commonly used method to determine pK_a values from the titration curves (Fig. 4) includes [27], the second derivative (Δ^2pH / Δ^2V) and the diagram of distribution of ionic species. As shown in Fig. 4A where the volumes of NaOH and HCl solutions added are designated positive and negative, respectively, using the nonlinear regression (NLR) method [28,29] shows three levels and suggests the existence of three pK_a values. The third pKa value is simply due to the neutralization of the stabilizing diisopropylammonium cation (*i*$Pr_2NH_2^+$), which has an acidic character, by the excess of NaOH.

The second derivative method ($\Delta^2pH / \Delta V^2$) will be mainly applied to the determination of the pK_{a1} = 3.6 and pK_{a3} = 7.5 values of *i*Pr_2NH_2-MA from the titration curves because of its convenience and its precision (Fig. 4 B). This method does not make it possible to clearly distinguish the value of pK_{a2}. However, the diagram of distribution of ionic species as a function of pH method could be used to determine this pKa value. Fig. 4 C represents the distribution diagram of ionic species obtained by caculating the molar fraction (Xi) for each added volume of HCl and NaOH during the metric pH assay. This technique highlights the protonation and deprotonation equations of the *i*Pr_2NH_2-MA and makes it possible to find the pK_{a1} and pK_{a2} values which are respectively around 3.65 and 6.75 [30]. The results indicate that the second derivative (Δ^2pH / Δ^2V) and the ionic distribution diagram methods are capable of determining pK_{a1} with an error difference of ± 0.05 while an analysis error of ± 0.2 exist for pK_{a2} using the NLR and the ionic distribution diagram methods. These pK_a values, corresponding to

UNDER PEER REVIEW

the ionization of the different sites (carboxylate, carboxylic and ammonium) of *i*Pr_2NH_2-MA, are close to those of the maleate derivatives [31].

For this, it would be interesting to confirm these pK_a values, hence the use of the conductimetric technique.

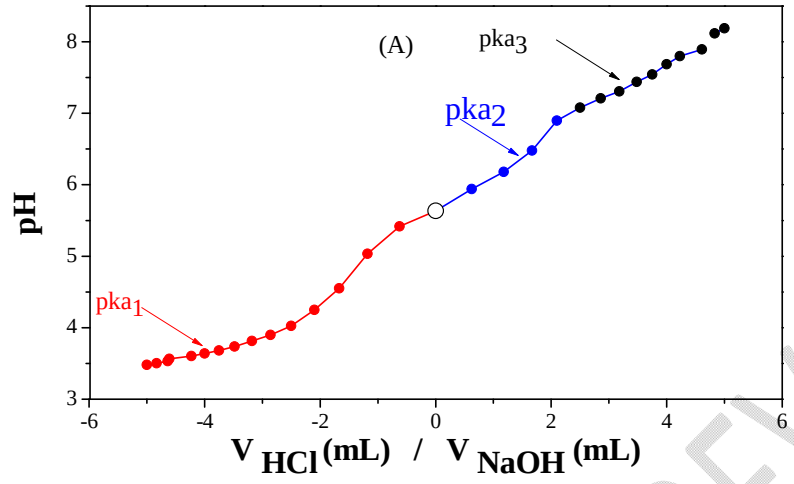

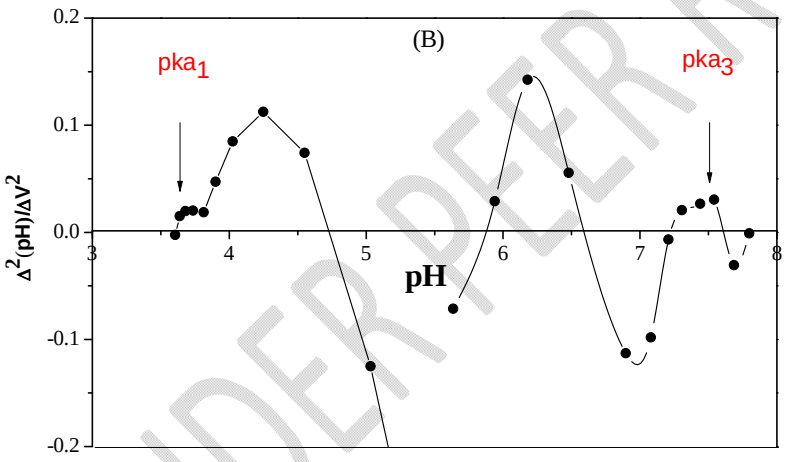

UNDER PEER REVIEW

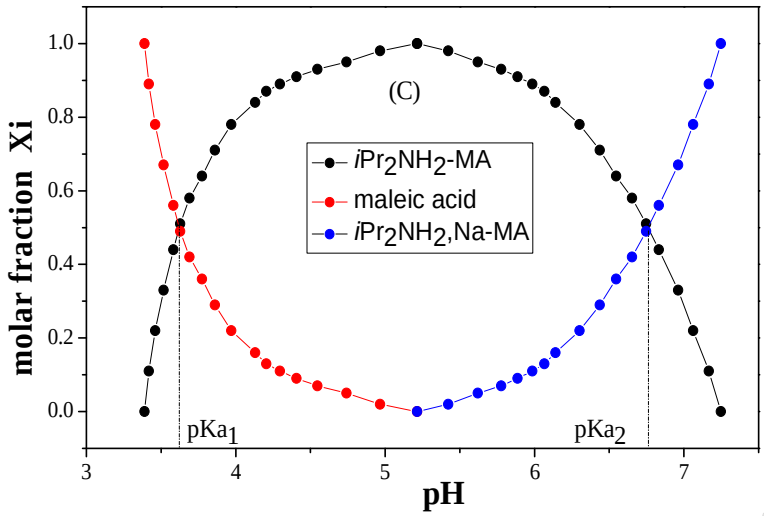

Fig. 4. Titration of *i*Pr_2NH_2-MA (10^{-4} M). (A): titration curve, (B): Curve of the second derivative, C): Diagram of distribution of ionic species as a function of pH.

3.5.1.2 Conductometric method

This method consists in simultaneously measuring of the conductivity and pH values (during titrations with HCl and NaOH) allowing the plot of α vs. f (pH) curves and the determination of pK_a values. In fact, according to the Henderson Hasselbalch (HH) equation (1), this result leads the relationship between the measured pH and the dissociation coefficient α [32].

$$pH = pK_a + \log\frac{[A^-]}{[AH]} \qquad \text{(Eq.1)}$$

$[A^-]$ and [AH] are the concentrations of dissociated acid and non-dissociated acid, respectively (we suppose here that the activity coefficients are close to 1).

The degree or coefficient of dissociation α of acids is defined as follows:

$$\alpha = \frac{[A^-]}{[AH]+[A^-]} \qquad \text{(Eq.2)}$$

$$\text{(1) and (2)} \Rightarrow \quad pH = pK_a + \log\frac{\alpha}{1-\alpha} \qquad \text{(Eq.3)}$$

$$\text{Furthermore } \alpha = \frac{\Lambda}{\Lambda_0} \qquad \text{(Eq.4)}$$

$$\text{and } \Lambda = \frac{\sigma}{1000\bar{C}} \qquad \text{(Eq.5)}$$

$$\bar{C} = \frac{CV - C'V'}{V_T} \qquad \text{(Eq.6)}$$

UNDER PEER REVIEW

In this case, knowing the conductivity σ (measured) and the concentration ($\overline{C}$) (calculated from Eq.6 after each addition of well-defined titrating solutions), we can deduce the value of the molar conductivity Λ. The value of Λ_0 is an unmeasurable quantity, but can be obtained by extrapolation in a graph of Λ as a function of the molar concentration, as illustrated in Fig. 5. The known values of Λ_0 allow plotting the pH curves as a function log $\frac{\alpha}{1-\alpha}$ (Fig. 6). By considering the value of pH at α = 0.5, pK_{a1} and pK_{a3} can be obtained as 3.51 and 7.80 respectively. These pK_a values are very close to those found by the pH-metric method.

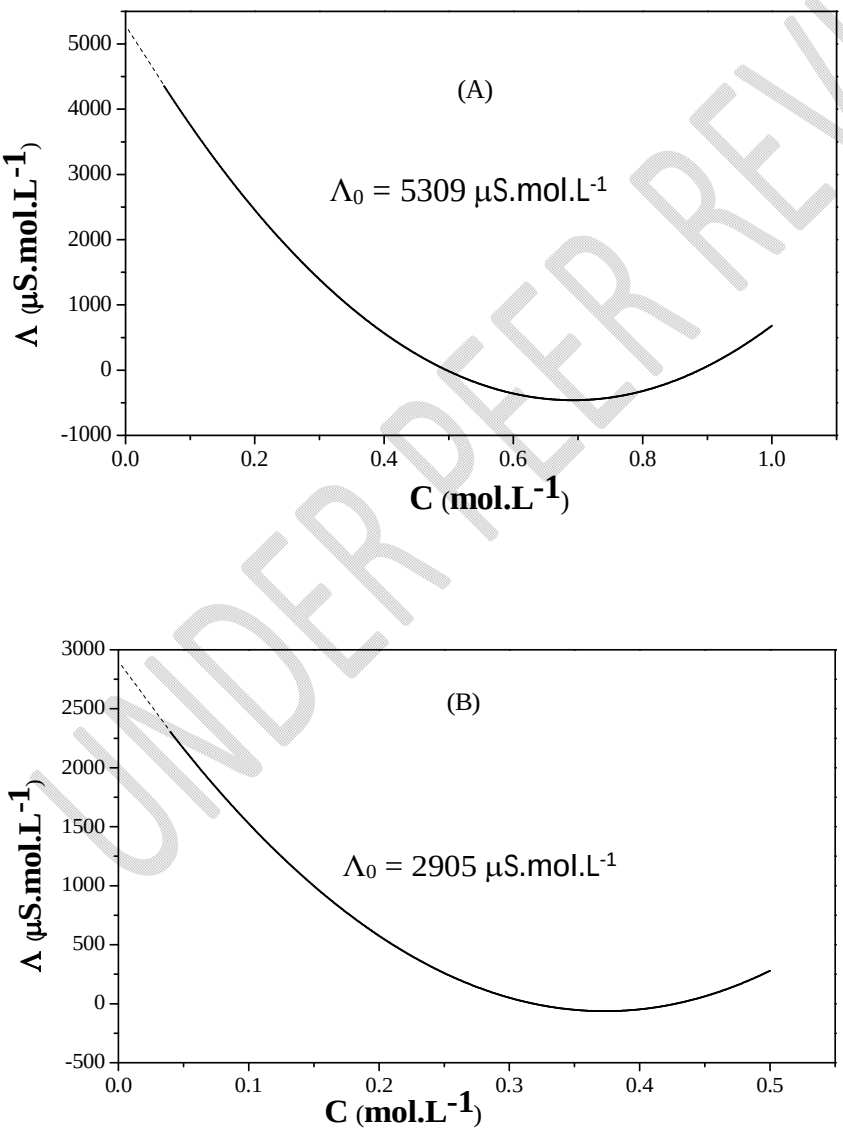

UNDER PEER REVIEW

Fig. 5. Curve Λ = f (C) of the iPr_2NH_2-MA titration by: A) 10^{-3} mol.L^{-1} HCl, B) 10^{-3} mol.L^{-1} NaOH.

Knowing that $\alpha = \frac{\Lambda}{\Lambda_0}$ and $pH = pK_a + \log\frac{\alpha}{1-\alpha}$, the curve $pH = \log\left(\frac{\alpha}{1-\alpha}\right)$ can be plotted for each titration (with HCl and with NaOH).

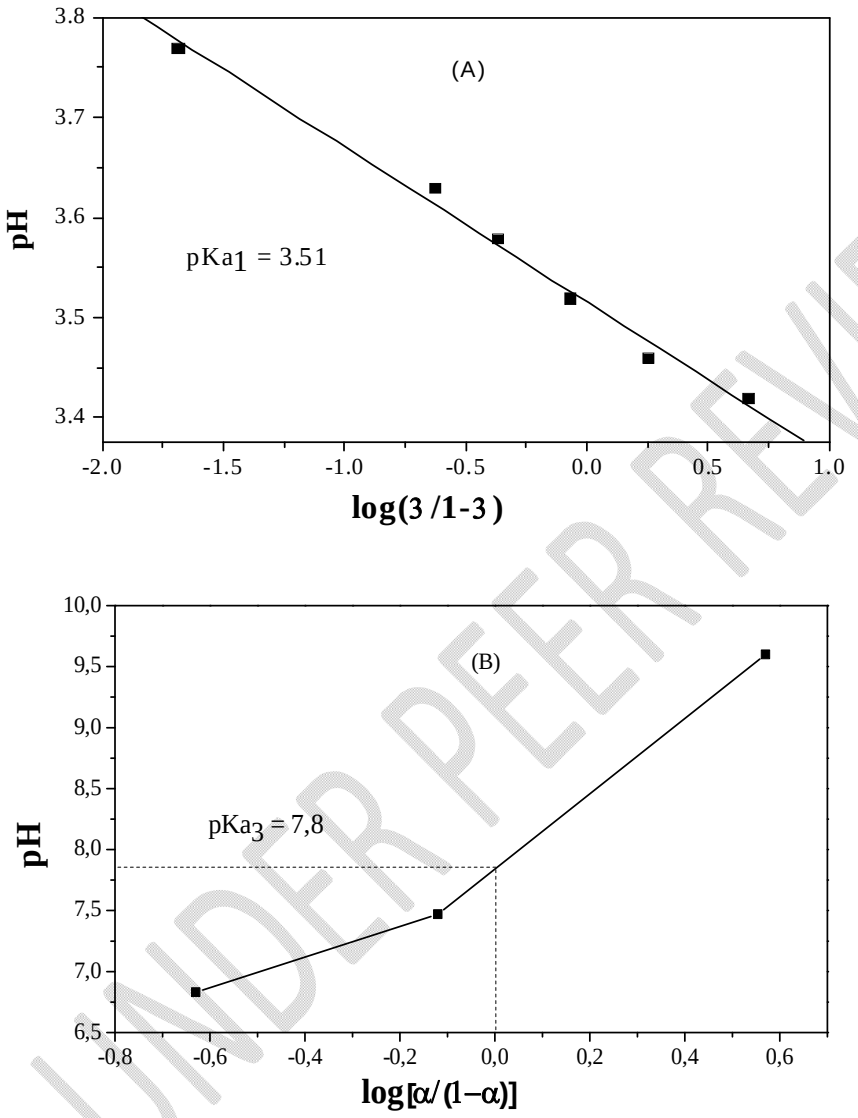

Fig. 6. pH = f($\log\left(\frac{\alpha}{1-\alpha}\right)$) for iPr_2NH_2-MA titration with: A): 10^{-3} mol.L^{-1} HCl, B): 10^{-3} mol.L^{-1} NaOH

3.5.2 Methods validation for pKa values determination

The pK_a values have been determined by the pH-metric and conductimetric techniques. Only pK_{a1} and pK_{a3} value can be determined by all these techniques. However, using the RNL methods, Δ^2pH / Δ^2V = f (pH), Xi = f (pH) an error of the order of ± 0.01 is observed for the values of pK_{a1}. On the other hand, only the pH-metric technique (NLR, Xi = f(pH)) makes it possible to determine the value of pK_{a2}. These

UNDER PEER REVIEW

results show that the pK_a values in an aqueous medium of the molecules can be determined with precision and simplicity using these different techniques.

The pKa values were calculated at three different concentrations of *i*Pr_2NH_2-MA for each method. The linearity of the curves pH = f ($\log\frac{\alpha}{1-\alpha}$) was evaluated by a variance analysis [33]. In all cases, the regression variance (V_{REG}) is significantly higher than the residual variance (V_{RES}) (P-value =.0005), which shows that the regression is significant and that the linear model is validated (Table 1).

To validate the pKa values obtained by the linear regression, a comparison was made by a Student t-test. In order to show the practical interest of the linear regression method for the determination of pKa values, we have also done triplicates test points, at α values different from those used of the linear regression curves. The tabulated Student t value (confidence level of 5%) is higher than the calculated t of the difference (t_D), which shows that there are no significant differences between the results obtained for the Student's t tests and the pKa values obtained from the linear regression curves (Table 1).

Table 1. Evaluation of the pKa values by variance analysis at a confidence level of 5% and by a Student t-test

Linear regression method	**pH = $pK_a + \log\frac{\alpha}{1-\alpha}$**	**pKa_1**	**pKa_2**	**pKa_3**
pKa values		3.51±0.06	6.81±0.02	7.80±0.18
ANOVA 1				
	Regression variance (V_{REG})	44.96	134.87	96.64
		0.34	0.11	1.23
	Residual variance (V_{RES})	0.00	0.00	0.00
	P value			
Student t-test		pKa_1	pKa_2	pKa_3
	pKa	3.49**±0.02**	6.55**±0.36**	7.64**±0.22**
	t_D	0.02	0.25	0.16
	t_S	89.47	31.88	153.15
	SD	NO	NO	NO

SD (pKa): Standard deviation of the pKa.
t_D: Calculated Student value of the difference between the two pKa.
t_S: Tabulated Student t value.
SD: Significant difference

UNDER PEER REVIEW

3.5.3 Determination of thermodynamic parameters

The value of the enthalpy (ΔH) was estimated from the equation of Van't Hoff [34-36]. We assumed that $\Delta_r H^0$ and $\Delta_r S^0$ are not temperature dependent [37-39].

$$\frac{d}{dT}\ln K = \frac{\Delta_r H^0}{RT^2} \quad \text{(Eq.7)}$$

Where $\Delta_r H^0$ is the standard enthalpy change of the acidic dissociation reaction, K the equilibrium constant, R the universal gas constant (8.31 J mol^{-1} K^{-1}) and T the absolute temperature.

The standard entropy change $\Delta_r S^0$ was derived from standard Gibbs free energy and enthalpy changes [39,40]. Gibbs free energy and entropy can be expressed as follows:

$$\Delta_r G^0 = -RT\ln K \quad \text{(Eq.8)}$$

$$\Delta_r S^0 = -\frac{\Delta_r G^0 - \Delta_r H^0}{T} \quad \text{(Eq.9)}$$

Finally, Van't Hoff's equation can be rewritten:

$$\ln K = -\frac{\Delta_r H^0}{R}\cdot\frac{1}{T} + \frac{\Delta_r S^0}{R} \quad \text{(Eq.10)}$$

Taking into account the relation K a = $[H_2O]$ * K = 55,55x K, we obtain:

$$\Rightarrow \quad pKa = \frac{\Delta_r H^0}{2{,}303*R}\cdot\frac{1}{T} - \frac{\Delta_r S^0}{2{,}303*R} - 1{,}74 \quad \text{(Eq.11)}$$

The curves pKa_1 as a function of $T^{-1}$are shown in Figure 7, and these curves were examined by variance analysis (as explain in paragraph 3.5.2). In all cases, the regression is significant, without lack fit (at 5% confidence level), meaning that the linear model is validated.

The slope (a) and the intercept (b) obtained from these linear curves have been used to determine $\Delta_r S^0$ and $\Delta_r H^0$ (Fig. 7), and the standard Gibbs free energy (ΔG^0) can be determined at a specific temperature using equation (Eq.9).

For *i*Pr_2NH_2-MA, three samples were used which S_1, S_2 and S_3 solutions with concentrations of 10^{-3} $mol.L^{-1}$, $1.4x10^{-3}$ $mol.L^{-1}$ and $4x10^{-3}$ $mol.L^{-1}$, respectively. The pK_a values were calculated at different temperatures (298-323 K) for each solution.

The calculated values of the standard enthalpy, entropy and Gibbs free energy of iPr_2NH_2-MA dissociation are given in Table 2 for the S_3 solution. It appears that pK_a values decrease with increasing temperature. These results are similar to those of El-Bindary [41], which justifies the acidity of *i*Pr_2NH_2-MA increases with increasing temperature. The values of $\Delta_r H^0$ are 25.36 ± 0.06 kJ mol^{-1} K^{-1} indicate that dissociation is endothermic.

The positive ΔrG^0 values have been obtained in the temperature range (298-323 K). As ΔrG^0 does not allow a priori to predict the evolution of the system, it is ΔrG which plays this role. However, if ΔrG° is very positive, it is likely that ΔrG is too. Reasoning on ΔrG^0 (equilibrium condition) is therefore very likely to give a good prediction. Note that this type of reasoning is identical to that which consists in affirming that if an equilibrium constant is large the reaction takes place in the direct sense, if it is very small in the indirect sense. The low pka values and the positive ΔG^0 indicate that the dissociation

UNDER PEER REVIEW

process is very low in the direct sense, i.e. the protonation reaction of diisopropylammonium hydrogenmaleate in acidic medium is not spontaneous in the temperature range.

The decreases in ΔG^0 as a function of the temperature have shown that the dissociation of the *i*Pr_2NH_2-MA is favored by the increase of temperature. However, the values of $\Delta_r S^0$ are 6.08 J.mol^{-1}.K^{-1} due to increased disorder as result of the dissociation processes. All these thermodynamic parameters of *i*Pr_2NH_2-MA confirm the stability of the crystalline molecule in aqueous medium.

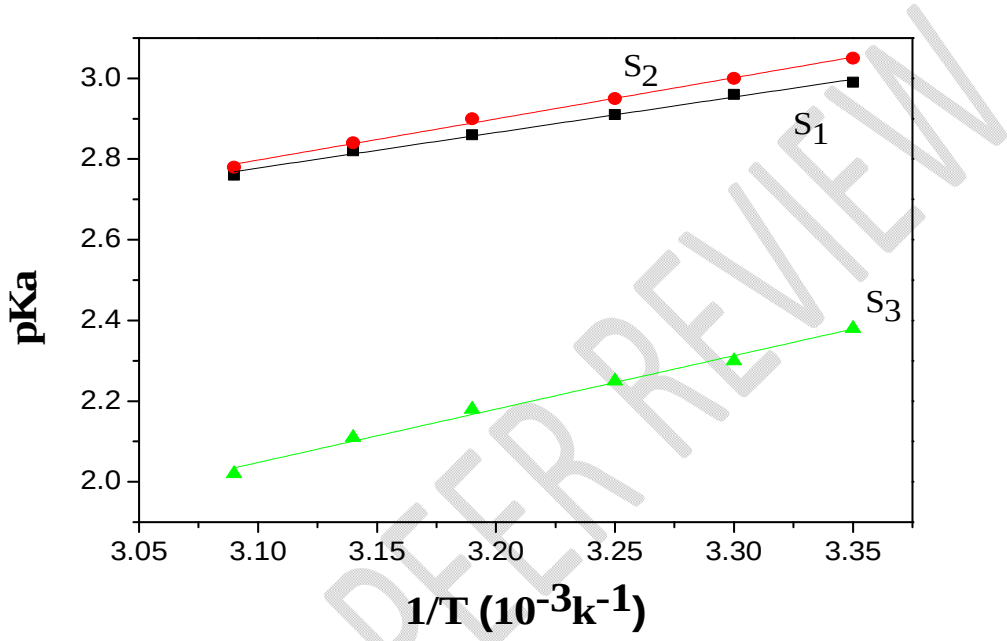

Fig. 7. pK_a vs. 1/T for *i*Pr_2NH_2-MA solutions at different concentrations: 10^{-3} mol.L^{-1} (S_1), 1.4x10^{-3} mol.L^{-1} (S_2) and 4x10^{-3} mol.L^{-1} (S_3).

Table 2. The different values of thermodynamic parameters

ΔH (KJ.mol^{-1})	**ΔS (J.mol^{-1}. K^{-1})**	**Temperature (K)**	**ΔG (KJ.mol^{-1})**
		298	23.55±**0.02**
		303	23.52±**0.05**
ΔH = 25.36±0.06	**ΔS = 6.08± 0.18**	308	23.49±**0.03**
		313	23.46 ±**0.01**
		318	23.43 ±**0.12**
		323	23.40±**0.12**

UNDER PEER REVIEW

3.5.4 Determination of the solubility of iPr_2NH_2-MA.

The determination of the solubility of iPr_2NH_2-MA, which is an amphoteric salt, can be easily done using the solubility - pH curves from the HH equations [42].

Fig. 8 A represents the solubility as a function of the pH of the diisopropylammonium cation ($iPr_2NH_2^+$). This curve shows an intrinsic solubility value (S_0) of about 0.08 mg/mL which appears to be very limited. Between $iPr_2NH_2^+$ and the hydrogenmaleate anion leads to the formation of a salt with an intrinsic solubility value of around 1.33 mg/mL (Fig. 8B). These different values showed an improvement in the intrinsic solubility S_0 starting from the free form in the saline state. These results demonstrate the central role of the maleate anion in the design of molecule for improving solubility.

The maximum solubility value S_{max} = 84 mg/mL of iPr_2NH_2-MA, classified as a soluble product according to European Pharmacopoeia, was found to be excellent compared to the solubility values of other molecules approved by the Administration of Medication Food (ANM) such as Ethionamide maleate (S_{max} = 19.9 mg/mL in acidic medium) [18], choline febuxostat (CXT) (S_{max} = 30 mg/mL in water) [24].

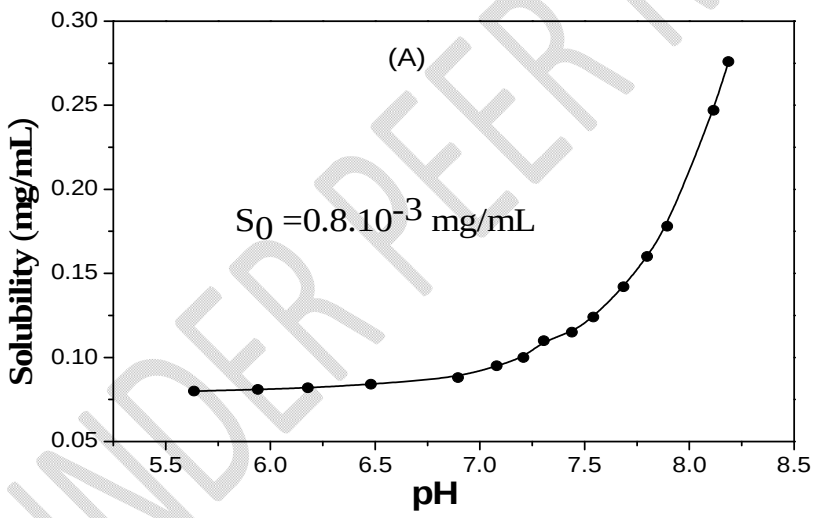

UNDER PEER REVIEW

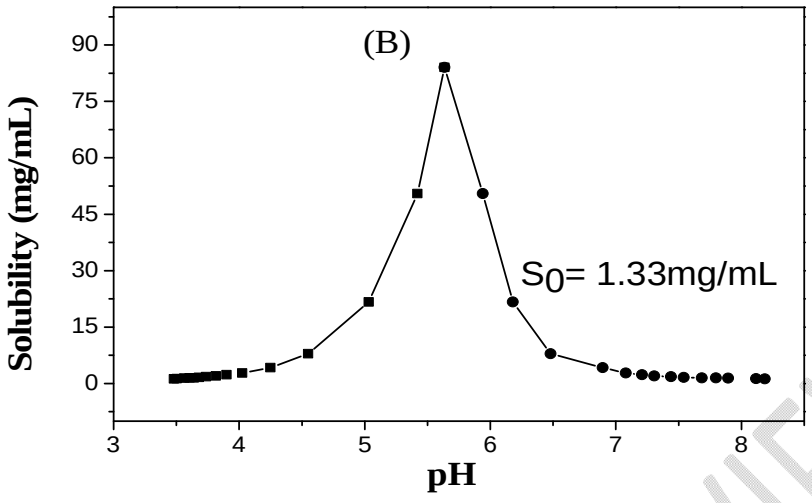

Fig. 8. Solubility vs. pH for *i*$Pr_2NH_2^+$ (A), and *i*Pr_2NH_2-MA salt (B).

UNDER PEER REVIEW

4. Conclusion

In this study, the values of pK_a, solubility, and thermodynamic parameters of a new crystalline molecule *i*Pr_2NH_2-MA were determined. Due to their simplicity and accessibility, conductimetric and pH-metric methods have been used in order to be able to know the physicochemical properties of the molecule. At the end of our study, it turned out that the pH-metric titration makes it possible to determine the amphoteric nature of the *i*Pr_2NH_2-MA molecule and this was confirmed by the conductimetric method. These methods allowed us to calculate the physico-chemical parameters of the molecule. The pK_a values very precisely evaluated, the thermodynamic parameters and solubility value showed that the dissociation of the crystalline molecule was spontaneous, endothermic and entropically favorable. The positive value of ΔG demonstrated that the stability of the *i*Pr_2NH_2-MA decreases with increasing temperature. This study shows the inexpensive implementation of the synthesis and the determination of the physicochemical parameters of a new *i*Pr_2NH_2-MA that could be potential active pharmaceutical ingredients.

Disclaimer (Artificial intelligence)

Option 1:

Author(s) hereby declare that NO generative AI technologies such as Large Language Models (ChatGPT, COPILOT, etc.) and text-to-image generators have been used during the writing or editing of this manuscript.

REFERENCES

1. Banerjee R Bhatt PM Ravindra NV Desiraju GR (2005) Saccharin Salts of Active Pharmaceutical Ingredients Their Crystal Structures and Increased Water Solubilities Cryst Growth Des 5:299-2309

2. Hathout RM Gad HA Abdel HSM Nasser N Khalil N Ateyya T Amr A Yasser N Nasr S Metwally AA (2019) Gelatinized core liposomes: A new Trojan horse for the development of a novel timolol maleate glaucoma medication. Int J Pharm 556:192-199

3. Nagori BP Maru A Muysuniand P Gupta S (2011) Method Development and Its Validation for Simultaneous Estimation of Timolol Maleate and Dorzolamide Hydrochloride in as API and in Ophthalmic Solution Dosage Form by RPHPLC. J Chem Pharm Res 3: 866-874

4. Bibi R Naqvi BS Shoaib MH Rahim N (2011) Design and evaluation of a new formulation of enalapril maleate tablet. J Pharm Sci 24:211-215

5. Tripathi J Gupta S Mishra B B (2024) Synthesis of guar gum maleate under dry conditions: Reaction kinetics and characterization International Journal of Biological Macromolecules 267 : 131591-131599

6. Savchenko V Eckert S Fondell M Mitzner R Vaz da Cruz V Föhlisch A (2024) Electronic structure, bonding and stability of fumarate, maleate, and succinate dianions from X-ray Phys. Chem. Chem. Phys 26 : 2304-2311

7. Tesfaye E Woldegiorgis F Eticha T Ashenef A (2024) Quality of medicines for Cardio-Vascular Diseases (CVDs) in the Ethiopian border with Kenya: The case of enalapril maleate and furosemide tablet quality in Borena and Gedeo zones PLOS Global Public Health 4: e0003104- e0003114

8. Zimmermann L Lee H L, Koishybay A Koishybay A, Cornelis P. VlaarJean-Christophe M (2024) Measurements and Correlation of Timolol Maleate Solubility in Biobased Neat and Binary Solvent Mixtures Journal of Chemical & Engineering Data J. Chem. Eng. Data 69 : 2369–2379

9. Dasilva CC Martins FT (2019) Multiple conformations and supramolecular synthons in almost fifty crystal structures of the anti-HIV/HBV drug lamivudine. J Mol Struct 1181:157-170

10. Tan G, Yu S, Pan H, Li J, Liu D, Yuan K, Yang X, Pan W (2017) Bioadhesive chitosan-loaded liposomes: A more efficient and higher permeable ocular delivery platform for timolol maleate. Int J Biol Macromol 94:355-363

11. Han GE, Priefer R (2023) A systematic review of various pKa determination techniques. Int J Pharm 635:122783

12. Sou T, Bergström CA (2018) Automated assays for thermodynamic (equilibrium) solubility determination. Drug Discovery Today 27:11-19

13. Shiung YC, Chen CY, Wu JC, Chang SW, Lin CH (2018) Determination of the pKa of Benzophenones by Capillary Zone Electrophoresis. J Chin Chem Soc 65:465-471

14. Albishri A, Cabot JM, Fuguet E, Rosés M (2022) Determination of the aqueous pKa of very insoluble drugs by capillary electrophoresis: Internal standards for methanol-water extrapolation. J Chromatogr A 1665:462795.

15. Sanli S, Sardogan S, Özdemir A, Atalay B (2022) Determination of Pka Values of Antidiabetic Drugs from Mobility Data and Pharmaceutical Analysis by Capillary Electrophoresis. J Chem Soc Pak 44:366-366

16. Mumcu A, Küçükbaya H (2015) Determination of pKa values of some novel benzimidazole salts by using a new approach with 1H NMR spectroscopy. Magn Reson Chem 53:1024–1030

UNDER PEER REVIEW

17. Pang J, Dou Z, Lin M, Xu W, Zhai S, Han Y, Wang J (2020) Mechanism of voltammetric determination of pKa of Bronsted–Lowry acids in aprotic solvent by quinone reduction. Microchem J 152:104324-104329
18. Barrientos C, Navarrete-Encina P, Carbajo J, Squella JA (2018) New voltammetric method useful for water insoluble or weakly soluble compounds: application to pK a determination of hydroxyl coumarin derivatives. J Solid State Chem 22:1423-1429.
19. Xiongwu W, Juyong L, Bernard RB (2017) Origin of pKa Shifts of Internal Lysine Residues in SNase Studied Via Equal-Molar VMMS Simulations in Explicit. Water J Phys Chem B 121 3318–3330
20. Babić S, Horvat AJM, Pavlović MD, Kaštelan-Macan M (2007) Determination of pKa values of active pharmaceutical ingredients Trends Anal Chem 26:1043-1063
21. Azzouz ASP, Ali RT (2018) Determination of pKa values for new Schiff bases derived from benzaldehyde and salicylaldehyde with glycine and ß- alanine. J Pure Sci 23 52 -61
22. Seye D Toure A Lo M Diop CAK Diop L Geiger D (2019) Crystal Structure of Diisopropylammonium Hydrogen Maleate. Sci J Chem 7(6): 110-113
23. Yan C Wu X-Y Luo O-Y Su L Ding Y-T Jiang Y Yu D-C (2019) Diisopropylamine dichloroacetate alleviates liver fibrosis through inhibiting activation and proliferation of hepatic stellate cells. Int J Clin Exp Med 12 :3440-3448
24. De Melo CC, Da Silva CCP, Pereira CCSS, Rosa PCP Ellena J (2016) Mechanochemistry applied to reformulation and scale-up production of Ethionamide: Salt selection and solubility enhancement. Eur J Pharm Sci 8:149-156
25. Han X, Qi W, Dong W, Guo M, Ma P, Wang J (2016) Preparation optimization and in vitro–in vivo investigation for capsules of the choline salt of febuxostat. Asian J Pharm Sci 11 :715-721
26. Rub MA Azum N, Asiri AM, Alfaifi SYM, Alharthi SS (2017) Interaction between antidepressant drug and anionic surfactant in low concentration range in aqueous/salt/urea solution: A conductometric and fluorometric study. J Mol Liq 227:1–14
27. Huang K, Xu Y, Lu W, Yu S (2017) A Precise Method for Processing Data to Determine the Dissociation Constants of Polyhydroxy Carboxylic Acids via Potentiometric Titration. Appl Biochem Biotechnol 183:1426–1438
28. Meloun M Pilařová L, Bureš F, Pekárek T (2018) Multiple dissociation constants of the intepirdine hydrochloride using regression of multiwavelength spectrophotometric pH-titration data. J MolLiq 261:480-491
29. Qiang Z, Adams C (2004) Potentiometric determination of acid dissociation constants (pKa) for human and veterinary antibiotics. Water Res 38:2874–2890
30. Ke J, Dou H, Zhang X, Uhagaze DS, Ding X, Dong Y (2016) Determination of pKa values of alendronate sodium in aqueous solution by piecewise linear regression based on acid-base potentiometric titration. J Pharm Anal 6:404–409
31. Loftsson T, Thorisdóttir S, Fridriksdóttir H, Stefánsson E (2009) Enalaprilat and enalapril maleate eyedrops lower intraocular pressure in rabbits. Acta Ophthalmol 88:337–341
32. Reijenga J, van Hoof A, van Loon A, Teunissen B (2013) Development of Methods for the Determination of pKa Values. Anal Chem Insights 8:53–71
UNDER PEER REVIEW

33. Rahim SA, Khan AJ1, Mazahar F (2020) Regression studies of binary complexes of bipyridyl with transition metal ions. Res J Chem Environ 24: 20-23
34. Abraha A (2016) Study Self-Association of Norfloxacin and Ciprofloxacin and their Thermodynamic Properties. J Pharm Sci Bioscientific Res 6:407-413
35. Shakeel F, Bhat MA, Haq N, Fathi-Azarbayjani A, Jouyban A (2016) Solubility and thermodynamic parameters of a novel anti-cancer drug (DHP-5) in polyethylene glycol 400 + water mixtures. J Mol Liq 229:241- 245
36. Geschwindner S, Ulander J, Johansson P (2015)Ligand Binding Thermodynamics in Drug Discovery : Still a Hot Tip. J Med Chem 58:6321−6335
37. Yang Z, Shao D, Zhou G (2020) Analysis of solubility parameters of fenbendazole in pure and mixed solvents and evaluation of thermodynamic model. J Chem Thermodynamics 140: 105876-105884
38. El Nahas S, Salman HM, Seleeme WA (2019) Aluminum Building Scrap Wire Take Out Food Container Potato Peels and Bagasse as Valueless Waste Materials for Nitrate Removal from Water supplies. Chem Afr 2:143–162
39. Bagwan UFR, · Teradale AB, · Shaikh IN, Harihar AL (2018) Kinetic Effect of Novel Osmium(VIII) for the Oxidation of Pyrazinamide by a Copper(III) Complex and Their Mechanistic Aspects. Chem Afr 1:53–66
40. Christian S, René H (2019) Exploring the Origins of Enthalpy−Entropy Compensation by Calorimetric Studies of Cyclodextrin Complexes. J Phys Chem B 123:6686−6693
41. El-Bindary AA, Mohamed GG, El-Sonbati AZ, Diab MA, Hassan WMI, Morgan SM, Elkholy AK (2016) Geometrical structure pH-metric molecular docking and thermodynamic studies of azo dye ligand and its metal complexes. J Mol Liq 218:138–149
42. Bergström CAS, Avdeef A (2019) Perspectives in solubility measurement and interpretation. ADMET & DMPK 7:88-105

UNDER PEER REVIEW